

Immersion Time and Annealing Temperature Effect on TiO₂ Thin Films Deposited by Hydrothermal Method

Selma M. H. Al-Jawad¹, Mohammad R. Mohammad¹ and Natheer Jamal Imran²

¹School of Applied Sciences, University of Technology, Baghdad-Iraq.

²Ministry of Science and Technology, Baghdad-Iraq.

Corresponding Author: 100069@uotechnology.edu.iq.

Abstract

In this work, TiO₂ nanofibers thin films were prepared by using different immersion times for hydrothermal method. Annealing in air at different temperatures of (400,500, and 600)°C at constant time (1 hour) were achieved for all films. Many analysis and measurement had been done (XRD, SEM, EDX, and AFM), and optical (UV-Visible spectroscopy, PL spectroscopy, and Spectral Response). The properties of nanofibers TiO₂ films were investigated and analyzed for films. The SEM analysis of TiO₂ films showed nanofibers shapes with diameter of about 21 nm. The absorption edges are located at UV-region, and the E_g has higher values compared with E_g for bulk TiO₂ film. Spectral response measurements show photocurrent peaks for TiO₂ nanotube films centered at UV-region (350 nm). [DOI: [10.22401/JNUS.20.3.11](https://doi.org/10.22401/JNUS.20.3.11)]

Keywords: TiO₂, hydrothermal technique, time of immersion effect, XRD, SEM, and AFM.

1. Introduction

The compound TiO₂ is n-type semiconductor due to oxygen vacancies, its conductivity increases with the degree of oxygen loss in the lattice. Titanium oxide thin film is one of the most studied transparent conductive oxides (TCOs) ^[1], because of its attractive physical, chemical and optoelectronic properties. It has good transmittance in the visible region, high refractive index, high dielectric constant, high photo catalytic activity (The photocatalytic activities of TiO₂ materials strongly depend on surface morphology, crystal structure, and crystallization of the concerned TiO₂ photocatalyst), chemical stability ^[2], non-toxic, inexpensive, easily synthesized, highly photostable, wide band gap ^[3], and good stability in various environments ^[4]. Furthermore, the surface of TiO₂ exhibits high hydrophilicity under ultraviolet (UV) light irradiation^[5].

There are three main types of TiO₂ crystalline structures: anatase, rutile, and brookite. Rutile presents the highest refractive index and is the most thermodynamically stable structure. It is also well known that titanium dioxide presents two isomorphous crystal phases; the anatase and the rutile ^[6]. The anatase structure is obtained at temperatures of around 300°C, which makes it more useful for industrial applications. At

temperatures between 400 and 600°C, the rutile phase is also present, while at higher temperatures, only the rutile structure is present^[7]. In general TiO₂ films transform from amorphous to anatase and then to rutile depending on the annealing temperature^[8]. However, some TiO₂ films from anatase contain small quantities of rutile phase and present a better efficiency than those of pure anatase^[9].

Nanometersized materials have recently gained a considerable attention to generate one-dimensional (1D) nanostructures such as nanotubes, nanowires and nanorods ^[10]. Because of their unique chemical and physical properties, such as a large surface to volume ratio, quantum size effect, efficient charge separation and transport properties^[11]. The porosity leads to a comparatively large internal surface area, which is advantageous for many applications where a good accessibility to the film surface becomes necessary. Porous materials as electrode material exhibit good electrochemical performance because these materials have both pores and high surface area which are adapted to the size of ions^[12]. The advance of product methods, in which the size, crystalline phase, and shape of the TiO₂ nanocrystals can be controlled, was of importance^[13].

In recent years, many studies related to the synthesis of nanostructures TiO₂ have been

focused on the control of particle size as well as morphology. Many deposition methods like anodic oxidation, hydrothermal, chemical vapor deposition, sol-gel, electron beam evaporation, chemical bath deposition (CBD), spray pyrolysis, successive ionic layer adsorption and reaction (SILAR), and electrodeposition are employing^[14]. It finds applications as photovoltaic cells, photocatalysis, dye sensitized solar cells (DSSC's), gas sensors^[15], lithium batteries, light waveguides^[16], water purification, self-cleaning surfaces, sterilization, biocompatible coatings, corrosion protection coatings, high permittivity dielectric layers for electronic devices^[17], and hydrogen generation by water photoelectrolysis^[18].

2. Experimental work

Hydrothermal synthesis was carried out using in a stainless steel Teflon lined autoclave; the Ti sheets were dived in a 15 ml H₂O₂(30wt-%) + 15 ml NaOH(10 M) solution inside the autoclave. Then, the autoclave was put in the oven at 80°C for different times of (8, 10, 12, 14, and 16) hours in order to start the hydrothermal synthesis and then cooled down until RT. Afterwards the Ti/TiO₂ sheets have been rinsed and dried. Later they were subjected to post treatments: acid washing and calcination. The acid washing was conducted through two cycles in 50 ml of low concentrated (0.1M) HCl solution for 2 hours each time. Finally the sheets were dried.

The crystal structure of TiO₂ films was analyzed by using x-ray diffraction system (Shimadzu XRD diffraction) with CuK α 1 radiation with $\lambda=1.54 \text{ \AA}$, at 30 kV, 30 mA. The films thickness was evaluated by TF ProbeTM Spectroscopy-Angstrom Sun Tech. Inc.-USA/model SR 300-2012. The morphologies of the resulting films were characterized by atomic force microscope (AFM) (CSPM-500 Csp M-5000 instrument, USA-20080) and scanning electron microscopy (SEM) (Hitachi Type S-4160), which operates at (20-30 KV) and (8000-60000 X) magnifications.

Annealing is carried out at different temperatures (400°C, 500°C, and 600°C) for one hour. To annealing films we use Carbolite® Shfld.-England Furnace. The optical transmittance and absorbance measurement were performed by using

Ultraviolet-Visible spectrophotometer (Phoenix-2000V/UV-VIS spectrophotometer / (Biotech Engineering Management Co., Ltd-UK), and Stellar Net. Inc. Spectroscopic Reflectometer-USA. All measurements were made at room temperature. Photoluminescence spectroscopy was done by VARIAN/CARY-Eclips-Fluorescence Spectrophotometer with Xenon flash lamp source.

The photoelectric method is one of the direct methods to determine absorption edge and band gap. The spectral response was performed using a monochromator with spectral (Lambda Scientific-model LEOI-94-grating monochromateor) .The current measurements were accomplished using Keithley 6517B electrometerl high resistance meter.

3. Results and Discussion

3.1. Structure and Surface Morphology Properties

The time of immersion in (NaOH+H₂O₂) solution is one of the critical parameters in the preparation process of fiber nanostructures.

The result of XRD characterization is in the form of X-ray diffraction patterns in Fig. 1(a-d), which shows that after preparation (immersion time was equal to 8 hour at 140°C) the film was amorphous and thus need to be annealed. After annealing at 600°C Fig.(1)(a(e)), peaks corresponding to TiO₂ phases are observed along peaks assigned to the titanium in the substrate, which are pronounced. Three main peaks at 25.25°-A(101) 48.25°-A(200), and 70.75°-A(220) are assigned to TiO₂ anatase phase and other stronger peaks attributed to the metallic Ti substrate. Note that the peaks corresponding to the anatase phase are broadened compared to those of Ti metal, suggesting the formation of smaller in size TiO₂ anatase crystals during the corrosion treatment of larger in size metal phase. Generally, nanofibers crystallize in the crystallographic structure of anatase forms only.

The splintering in the Ti peak $2\theta=70.85^\circ$ back to titanium plane (103) because the difference in the crystal structure between titanium metal and titanium dioxide semiconductors (the difference in the values of the lattice constants a, and c as well as the difference in the value of the angles β , γ , and

α) caused by two peaks one for titanium metal $2\theta=70.95^\circ$ - (103) and the other for TiO_2 $2\theta=70.75^\circ$ -A(220).

The evolution of X-ray patterns registered for TiO_2 nanofibers synthesized by hydrothermal methods (immersion time=16 hour at 140°C) is presented in Fig.(1)(b). After preparation, the TiO_2 as-deposited pattern Fig.(1)(b(d)) clearly shows very weak peak at $2\theta=25.4^\circ$ -A(101), characteristics of the TiO_2 anatase phase. And we can notice a beginning of splitting of main peak of Ti (103) to two peaks one of them is TiO_2 /A(220). After annealing at 600°C , XRD pattern of TiO_2 thin film is shown in Fig.1(b(e)), the pattern clearly shows

the peaks at 25.25° , 48.05° , and 70.6° corresponding to the lattice planes A(101), A(200) and A(220); characteristics of the TiO_2 anatase phase whereas other strong peaks can be assigned to the metallic Ti substrate. The anatase peaks are slightly wider than the metal peaks, confirming the formation of small oxide phase crystals during the hydrothermal treatment. Moreover it can be observed that the peaks obtained from the films deposited by time equal to 16 hours have increased in the intensities over the films deposited by time equal to 8 hours, demonstrating that increased deposition time will improve the structural properties of the TiO_2 thin films.

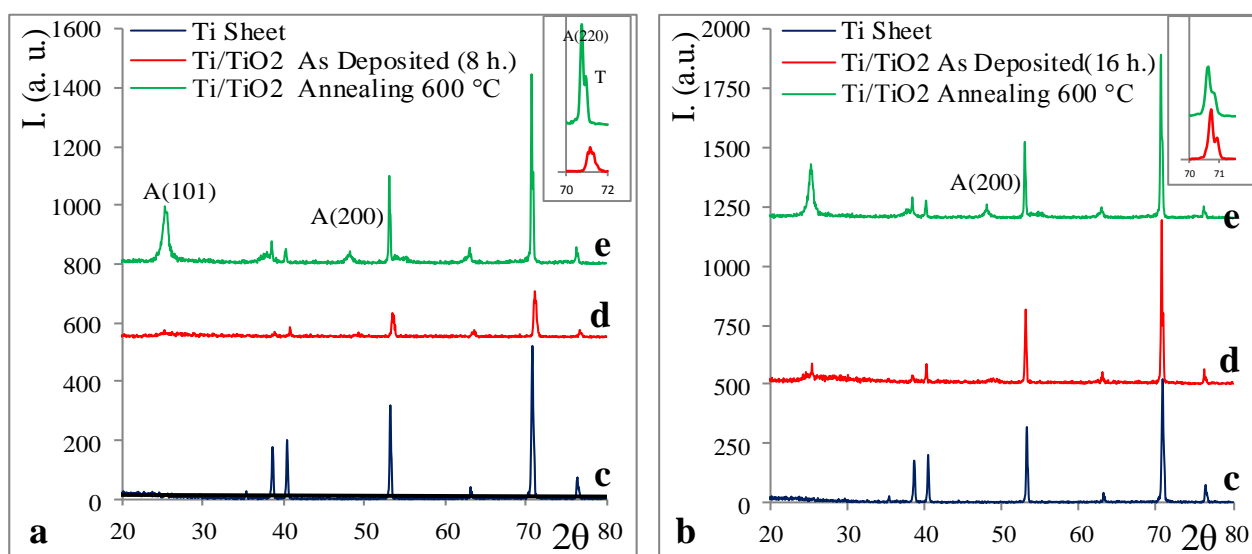


Fig.(1): XRD patterns of Ti/TiO_2 NFs thin film at different deposited times (a) $T=8$ h, (b) $T=16$ h (c) Ti substrate, (d) as-deposited, and (e) annealed at 600°C .

Fig.(2) shows a series of XRD patterns of the prepared TiO_2 by hydrothermal methods at 140°C (as-deposited and annealing at 600°C) at various immersion times (8, 10, 12, 14, and 16) hour. Fig.(1)(a), shows as-deposited films with different deposited time, the film (with deposited time=8 hour) shows amorphous structures, this means that the time used to deposit the film is not enough to make film polycrystalline structures. When deposited time arises to 10 hour Fig.(2)(a(d)) we can notice appearance of small diffraction peaks at $2\theta=25.25^\circ$ -A(101), characteristics of the TiO_2 anatase phase (this means transform in lattice structure from amorphous to polycrystalline. With increasing deposited time (immersion times), the peaks become bigger and broader with other peaks located in $2\theta=70.6^\circ$ /A(220) -

(JCPDS No.(21-1272). The hydrothermal synthesis route presents the advantage of obtaining phase-pure TiO_2 nanofibers at both lower temperatures and reaction times.

Fig.2(b), shows annealing films at 600°C , with different deposited times (8, 10, 12, 14, and 16) hour. All XRD patterns of the annealing films deposited in different times, showed complete formation of the crystalline anatase phase and are indexed according to the JCPDS card No. 21-1272. The nanocrystalline anatase structure was confirmed by $2\theta=25^\circ$ /A(101), 48° /A(200), and 70° /A(220), diffraction peaks. The widths of the bases of the peaks and their intensity characterize the size of the nanocrystals, because small crystals may promote a more intense spreading due to internal reflections that occur in the system.

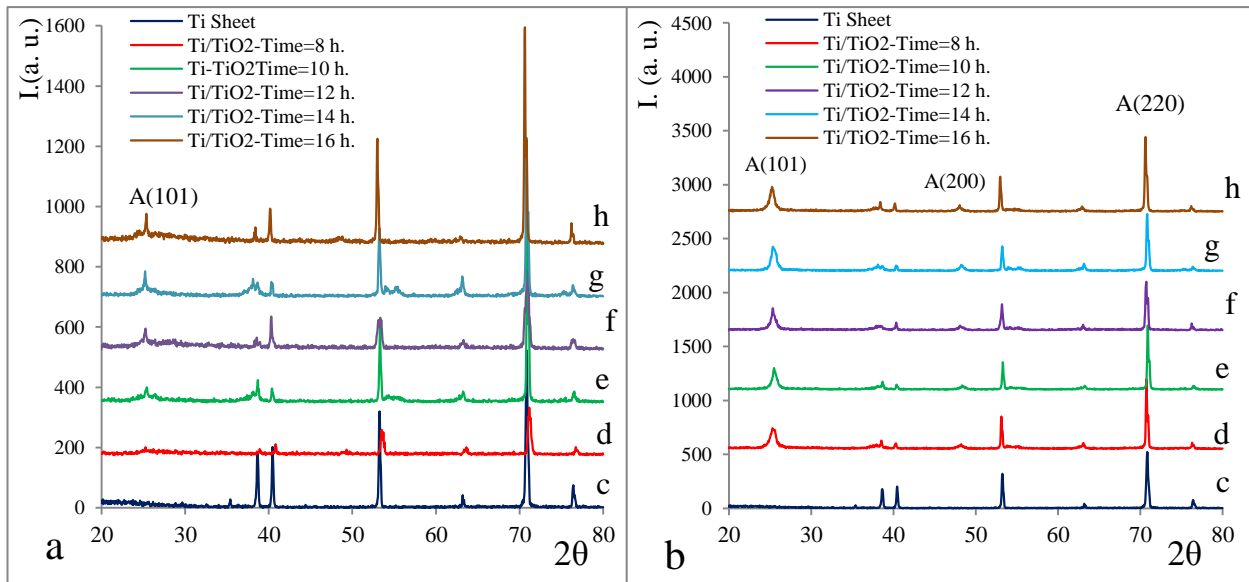


Fig.(2): XRD patterns of Ti/TiO₂ NFs thin films at different deposited times (a) as-deposited films (b) Annealed films at 600°C (c) Ti substrate, (d) 8 hours, (e) 10 hours, (f) 12 hours, (g) 14 hours, and (h) 16 hours.

Fig.(3)(a) shows the grain size with immersion times, a decrease is observed in the value of a grain size with an increase in immersion times and it is due to the improvement in the nanostructure of the films.

Fig.3(b), shows the micro-strain with immersion times, In general we note a decrease in the value of micro-strain.

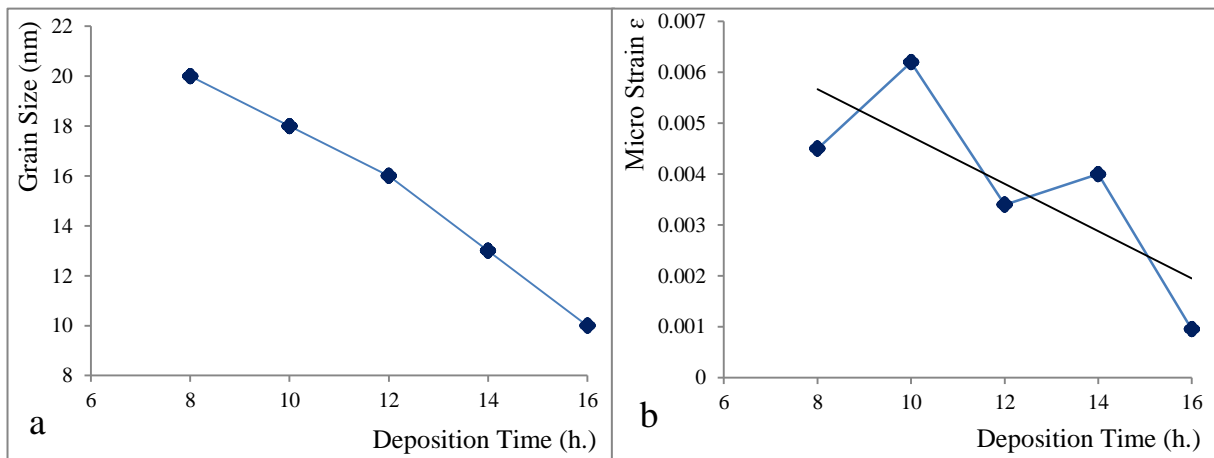


Fig.(3): The variation of (a) grain size, and (b) micro strain as a function of deposition time.

3.2. Scanning Electron Microscope (SEM) and EDX Analysis

The SEM images of as-deposited Ti/TiO₂ nanofibers (deposited by hydrothermal methods on Ti foil with 8 hours of immersion) and annealing at 600°C, are presented in Figure 4 with (60,000 X) magnification. The surface of titanium foil is etched and covered with Ti/TiO₂ NFs with diameter of about 25-29 nm. Moreover, Ti/TiO₂ nanofibers almost appear smooth surface and the formation is

incomplete Fig.(4)(a). The SEM image displays the film formed by overlapping and interpenetrating of the Ti/TiO₂ NFs.

The NFs stuck and interweaved, with many branches, just like a plant root.

The morphology of the branches, shown in Fig.(4)(a), is strongly dependent on the amount of time the nanofibers remain immersed in the (NaOH+H₂O₂) solution. As the immersion time increases, the branches become greater in number and longer in length. These branches

of TiO_2 nanofiber would greatly improve the specific surface area and roughness. Fig.(4)(b), shows Ti/TiO_2 nanofibers thin films annealing at 600°C , we can see increasing in the fiber thickness with diameter of about 27-32 nm.

We can also see the unfinished shape of nanofibers; due to the lack of time required to configure the appropriate shape (immersion time).

Fig.(5) shows SEM images of the surface of Ti sheets after hydrothermal treatment with immersion time=16 hour at (60.000 X) magnifications. One can notice that we have obtained a complex and more homogeneous structure made up of branched TiO_2 nanofibers Fig.(5)(a), then for film deposited in 8 hour of

immersion. The porosity offered by such structure is a good feature which permits easily including the CdS QDs during the further impregnation treatment. Moreover, the high surface to volume ratio of this structure allows a wider surface contact between the TiO_2 and the CdS. The TiO_2 nanofiber is more separated one than other and we have improvement in the fiber diameter (about ≈ 21 -23 nm). This recovery in nanofiber is due to the increasing in immersion time. Fig.(5)(b) shows Ti/TiO_2 nanofiber film annealed at 600°C . The diameter of fiber becomes thicker than as-deposited nanofiber film and diameter is about ≈ 25 -29 nm.

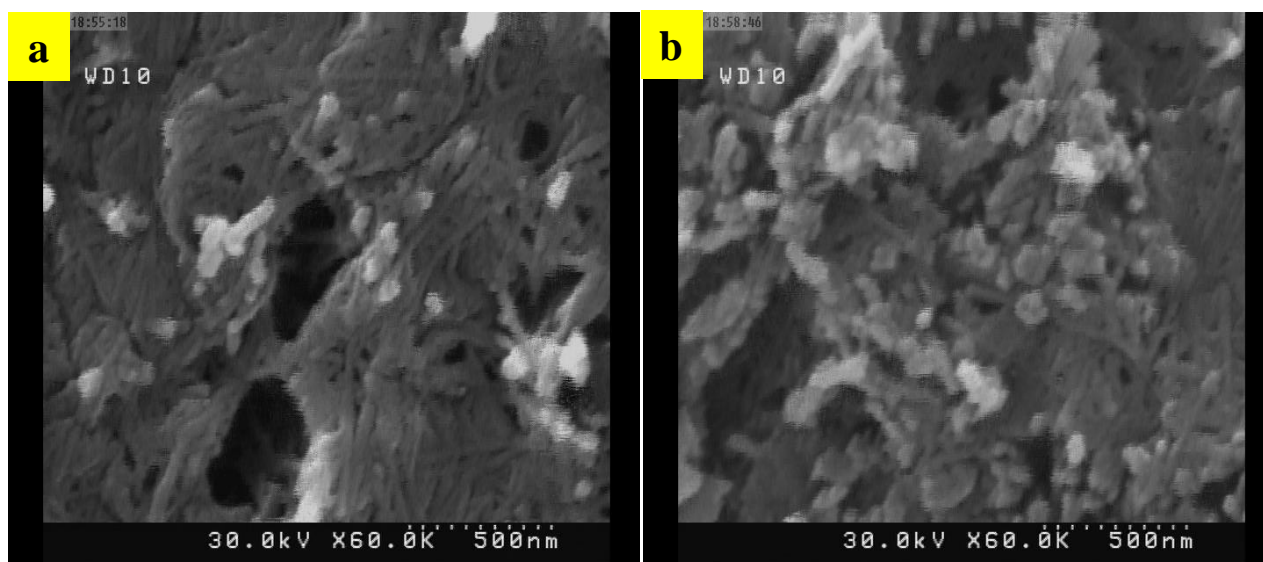


Fig.(4): SEM images of Ti/TiO_2 NFs thin film (a) as-deposited (Deposited Time= 8 h), and (b) annealed at 600°C .

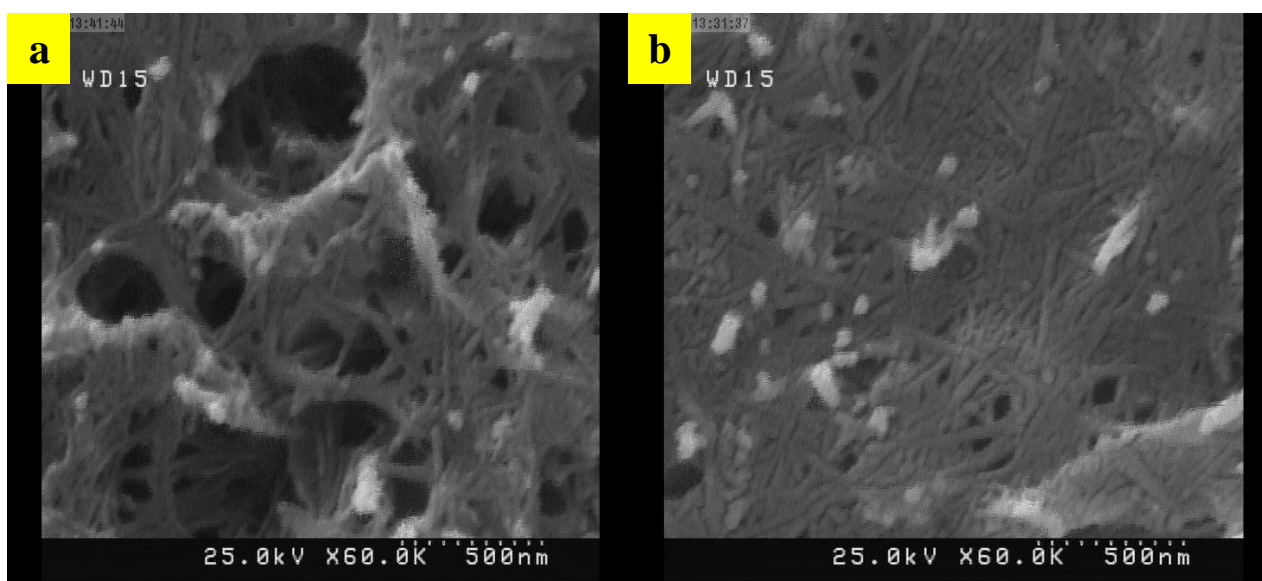


Fig.(5): SEM images of Ti/TiO_2 NFs thin film (a) as-deposited (Deposition Time= 16 h), and (b) annealed at 600°C .

Fig.(6) shows EDX analysis of the TiO_2 thin film (deposition time=16 h). EDX indicates that the film consists of titanium and oxygen elements. The ratio is about 28.96, and

71.04 respectively. These values are in agreement with the optimal stoichiometry for the sample.

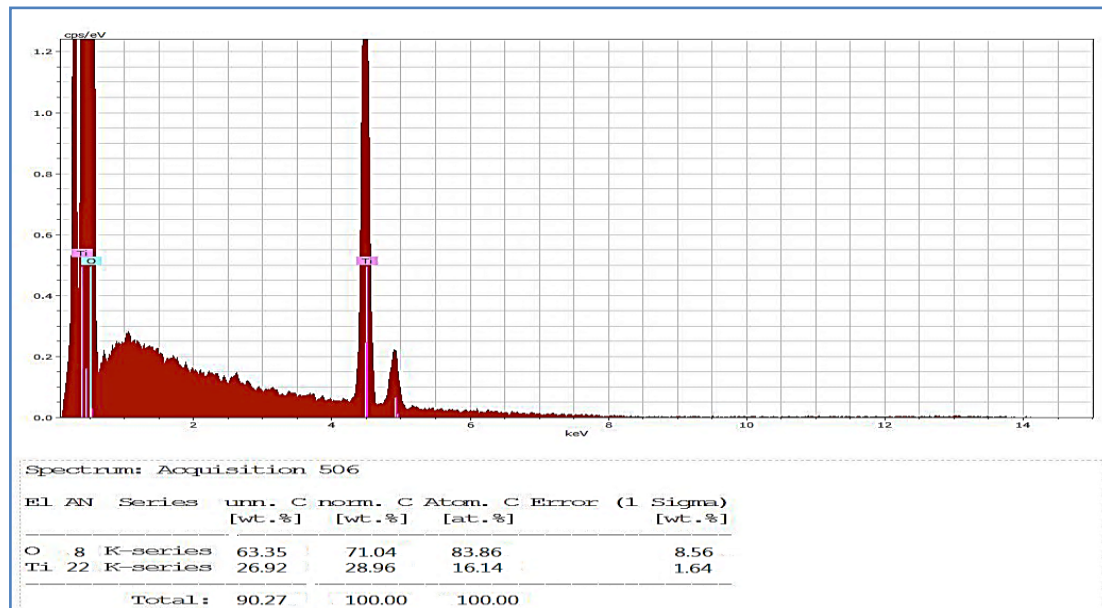


Fig.(6): EDX spectrum of Ti/TiO₂ nanofibers deposited by hydrothermal method.

3.4. Atomic Force Microscopy (AFM)

The surface morphology of Ti/TiO₂ NFs thin films (deposited time=16 h), was analyzed using atomic force microscope. Fig. 7(a) shows the typical three-dimensional AFM image of TiO₂ NFs, it can be see homogeneous surfaces morphology with fiber laid on surface and uniform distribution. AFM results show that average grain size to TiO₂ thin films about 72 nm, and the roughness average was about 2 nm. Root mean square (RMS) was 2.55 nm.

Fig.(7)(b), showed the granularity cumulation distribution chart of Ti/TiO₂ NFs.

3.5. Optical Properties

Optical absorbance, and energy band gap (E_g) spectrum of TiO₂ film (as-deposited and annealing at 600°C) on Ti (immersion time =8 hour) was shown in Fig.8. The both spectrum of TiO₂ films showed broad increase in absorption below 430 nm. A tailing absorbance in visible region of 500 to 700 nm was observed. The absorption edge was about ≈440, 445 nm for as-deposited and annealing films. The Fig.(8)(b), shows E_g of as-deposited and annealing films, and it can be notice reduction in the E_g values with annealing (due to slight enhancement in the lattice structure of film).The E_g values are

about 3.28, and 3.22 eV for as-deposited and annealed films respectively.

The UV-Vis. absorbance, and energy band gap (E_g) spectra of prepared samples by hydrothermal method (immersion time=16 hours) on Ti substrate Fig.(9), before and after annealing at 600°C. Fig.(9)(a) shows absorbance spectrum versus wave lengths for as-deposited and annealed films. Both spectrum lines show low stability in the high wave length and after 365 nm both lines have wide increment in the values (in region of low wave lengths). The absorption edge was found about 346, and 355 nm for as-deposited and annealed films (we can see red shift after annealing films and this is due to enhancement in the grain size of lattice structures). The E_g Fig.(9)(b), shows reduction in the values between as-deposited and annealed films of about 3.7 to 3.65 eV respectively.

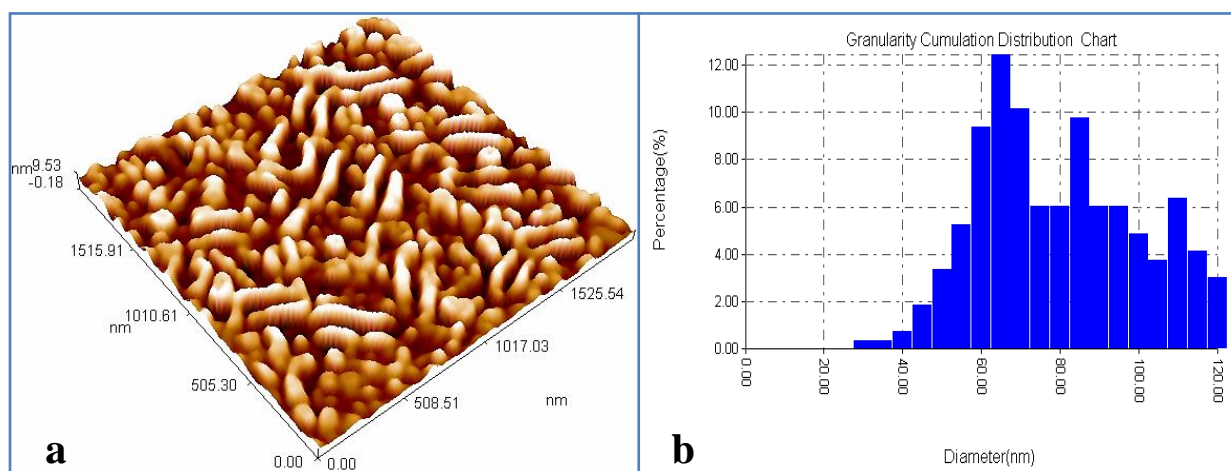


Fig.(7): (a) AFM image at 3D of Ti/TiO₂NFs thin film as-deposited ($T = 16$ h) on Ti sheet, and (b) granularity cumulation distribution chart.

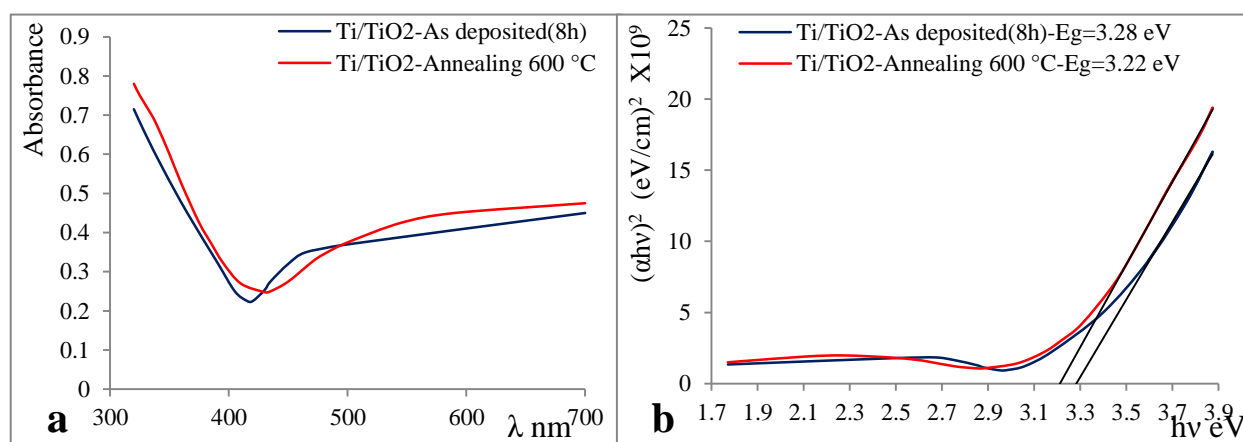


Fig.(8): (a) Absorbance spectra of Ti/TiO₂NFs as-deposited and annealing thin films (deposited time =8 h), and (b) Variation of $(\alpha hv)^2$ vs. (hv) for TiO₂ films.

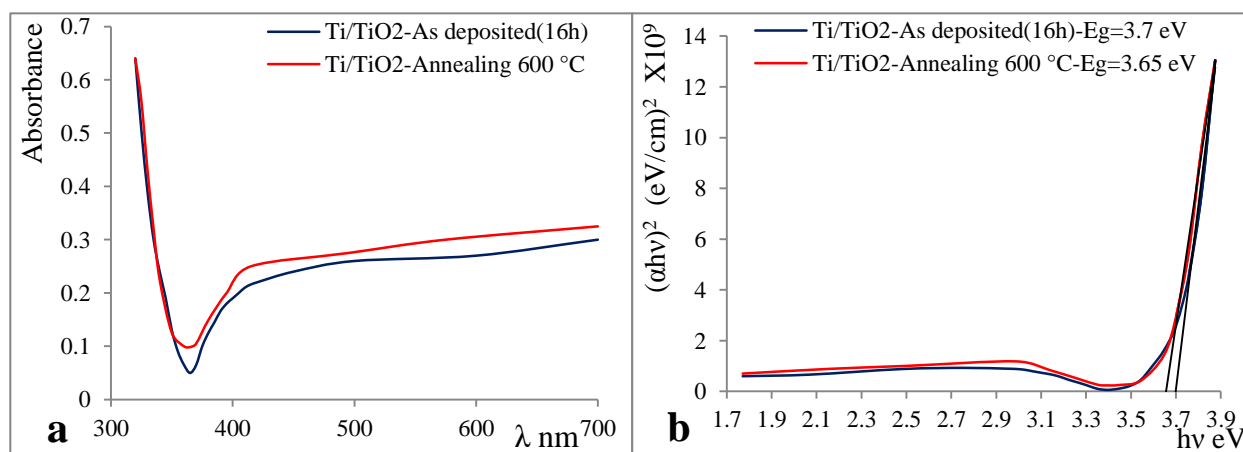


Fig.(9): (a) Absorbance spectra of Ti/TiO₂NFs as-deposited and annealing thin films (deposited time =16 h), and (b) Variation of $(\alpha hv)^2$ vs. (hv) for TiO₂ films.

The absorbance, and energy band gap (E_g) spectra for Ti/TiO₂ NFs as-deposited and annealed at 600°C films deposited at different times (8,10,12,14, and 16) are shown in Fig.(10).The absorbance spectrum lines versus wave lengths are shown in Fig.(10)(a), we can observe that the absorption edge values for all

spectrum lines have blue-shifted, with values about 440,403,382,368, and 345 nm for films deposited with time (8,10,12,14, and 16) hour respectively. We can explain blue-shifted by improving the nanostructures for films lattice (enhancement in the nanofibers for TiO₂ films). Fig.(10)(b) shows E_g values for all

deposited films. We can see increasing in the E_g values with increasing in the deposited time, the E_g values for deposited films are about 3.28, 3.4, 3.47, 3.6, and 3.7 eV for deposited time equal to 8, 10, 12, 14, and 16 hour respectively.

Fig.(10)(a'), shows absorbance spectrum lines for annealed films at 600°C with different deposited times (8, 10, 12, 14, and 16) hour. We see increasing in absorption edge values compared with as-deposited films, but for a same figure we can see also blue-shift in

the values. The absorption edge values were about $\approx 445, 415, 400, 375,$ and 355 for films with deposited time (8, 10, 12, 14, and 16) hours. These results might explain improving in lattice structures and nanofibers. The E_g values for annealed films are represented in Fig.(10)(b'), the values increase with increasing deposition time. The values were about $\approx 3.22, 3.37, 3.424, 3.56,$ and 3.65 eV for annealed films with deposition time = 8, 10, 12, 14, and 16 hours, respectively.

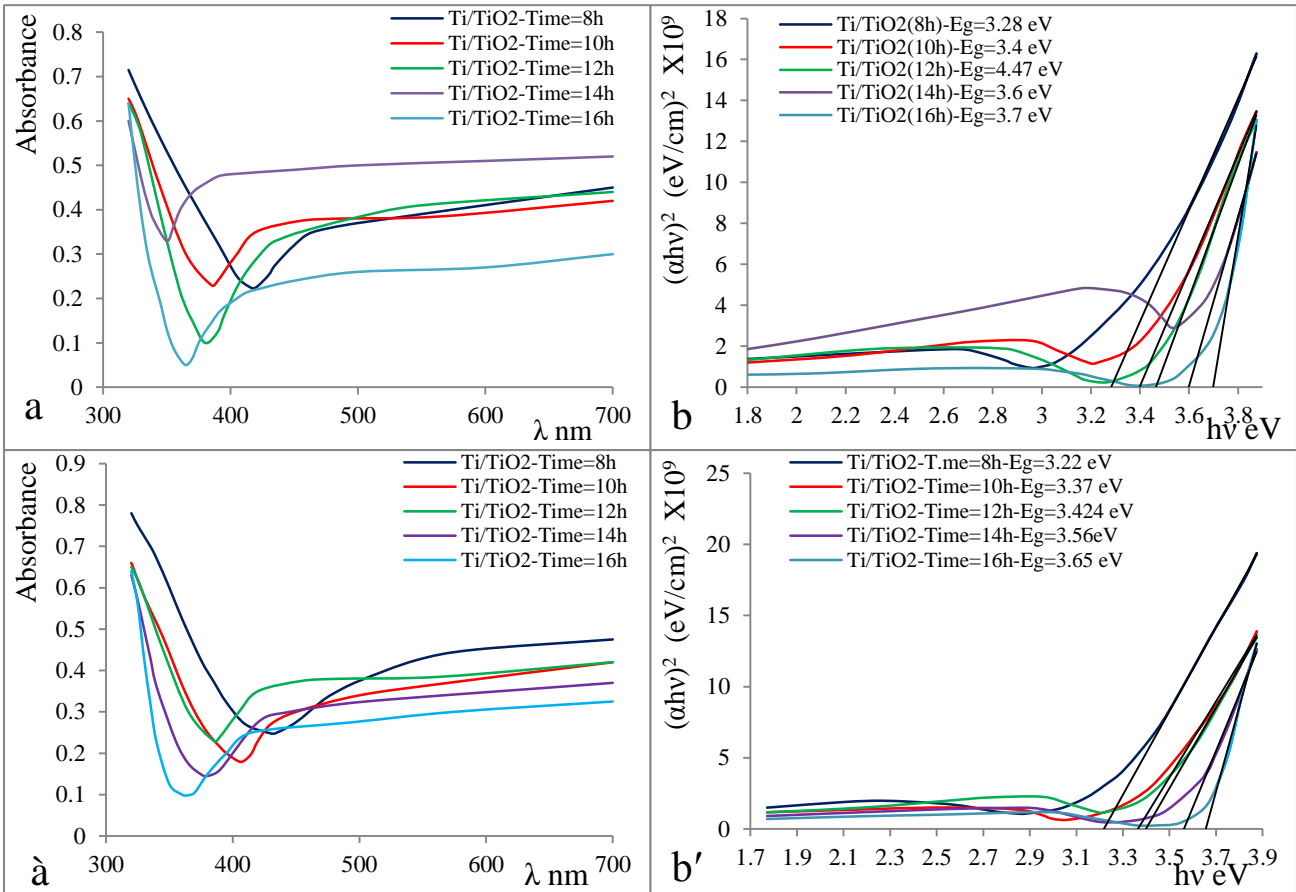


Fig.(10): Absorbance spectrum of (a) Ti/TiO₂ as-deposited thin films with different deposition time (time=8, 10, 12. And 16 h.) (a') annealing films at 600°C, (b) Variation of $(\alpha hv)^2$ vs. (hv) for TiO₂ as-deposited films (b') Variation of $(\alpha hv)^2$ vs. (hv) for annealing films at 600°C.

3.6. Photoluminescence Spectroscopy

Fig.(11) shows the PL spectra of the as-deposited and annealed Ti/TiO₂ NFs (immersion time=16 hours) with an excitation wavelength of 300 nm. It can be seen that as-deposited TiO₂ NFs Fig.(11)(a), shows an obvious two peaks, one at 340 nm (3.64 eV) and second's peak around 415 nm (≈ 3 eV). The emission around 345 nm corresponds to the near band edge emissions of the nanostructured TiO₂ NFs, while the peak is

around 415 nm may originate from the charge recombination on the deep level emission (DLE), shallow-trap surface states, and oxygen vacancies. Fig.(11)(b), shows annealing TiO₂ NFs, we can notice shift in the near band edge to become 345 nm (3.59 eV) with less broadening.

3.7. Spectral Response (SR)

The plot of spectral response for as-deposited Ti/TiO₂ NFs thin film (immersion time=16 h) on Ti substrate is shown in

Fig.(12). The photocurrent has a peak at wave length 350 nm which was observed, and it's close to optical edge for the same films. Also we can notice more there is increasing in the current, because of metallic substrates used in this experiment.

4. Conclusions

The XRD patterns for TiO₂ nanostructures thin films shows only anatase form for a films deposited by hydrothermal method. For Ti/TiO₂ NFs films by hydrothermal method we need more deposition time (immersion time) to obtain perfect nanofiber structure. FE-SEM images show the fiber diameter for Ti/TiO₂ nanofibers films is about 21 nm. EDX measurements show Ti to O ratio values result agreement with the optimal stoichiometry for the films. The determined optical band gap for TiO₂ nanostructures films shows direct

allowed transitions. And for all films have a large band gap, this are attributed to the contribution of quantum size effect and nanostructures form (the E_g values for bulk TiO₂ films about 3-3.2 eV). Therefore TiO₂ films absorb mainly the ultraviolet light. PL measurements for all TiO₂ nanostructures show two peaks in the spectrum range between 300-800 nm, one located at UV region and seconds' peak located in visible region. The emission in UV region corresponds to the near band edge emissions of the nanostructured TiO₂ films, while the peak in visible region may originate from the charge recombination on the deep level emission (DLE), shallow-trap surface states, and oxygen vacancies.

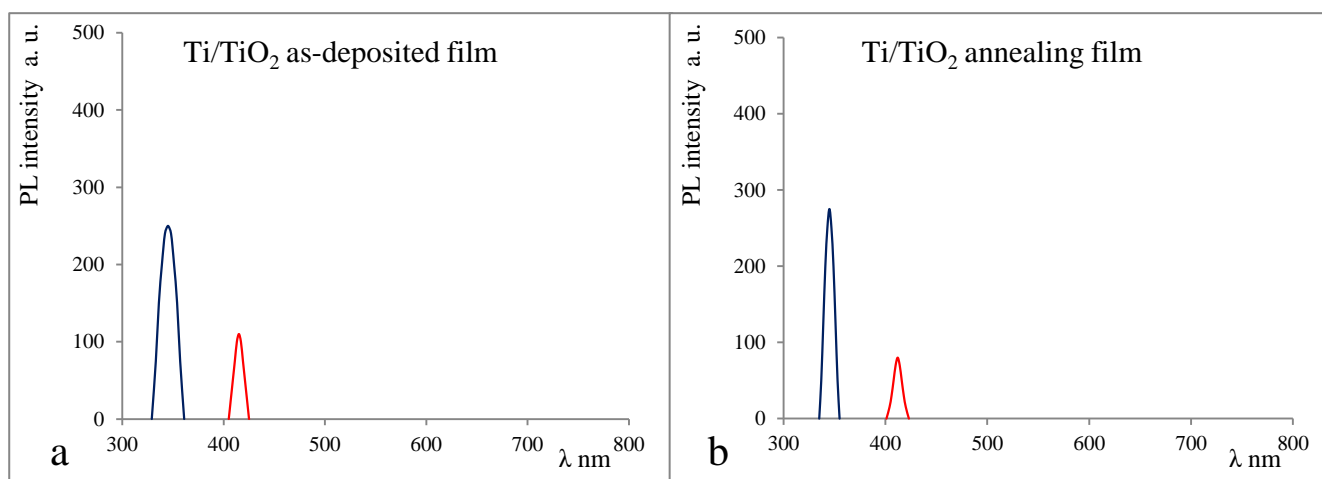


Fig.(11): Photoluminescence spectra of the (a) as-deposited, and (b) annealing at 600°C, Ti/TiO₂ nanofibers films on Ti sheet.

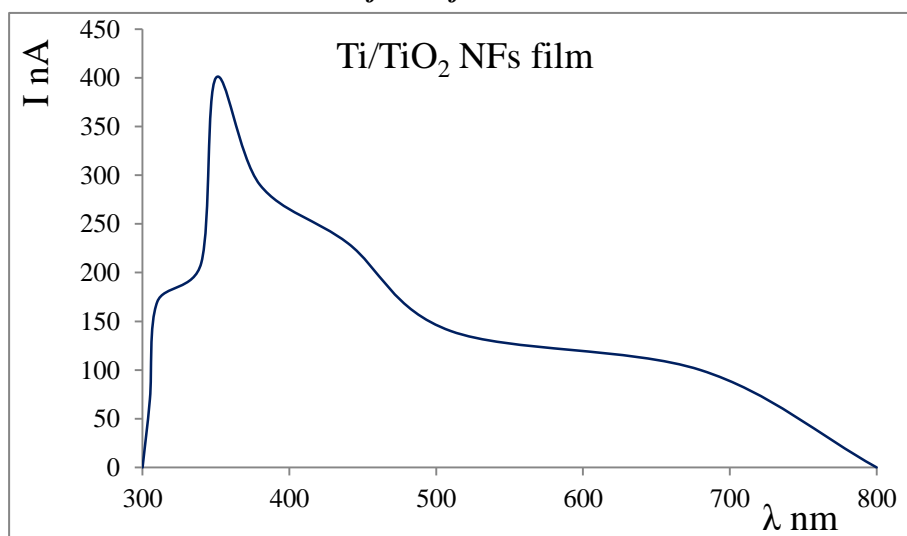


Fig.(12): Spectral response of as-deposited Ti/TiO₂ NFs thin films deposited by hydrothermal methods.

References

- [1] Igwe H.U., Ekpe O.E. and Ugwu E.I., "Effects of Thermal Annealing on the Optical Properties of Titanium Oxide Thin Films Prepared by Chemical Bath Deposition Technique", *Research Journal of Applied Science, Engineering and Technology*, 2(5), 447-451, 2010.
- [2] Li G-S., Zhang D-Q. and Yu J. C., "A new Visible-Light Photocatalyst: CdS Quantum Dots Embedded Mesoporous TiO₂", *Environ. Sci. Tech.*, Vol. 43, 79–85, 2009.
- [3] LEZNER M., GRABOWSKA E., and ZALESKA A., "Preparation and Photocatalytic Activity of Iron- Modified Titanium Dioxide Photocatalyst", *Physicochem. Probl. Miner. Process*, Vol. 48(1), 193–200, 2012.
- [4] A.M Gaur, R. Joshi, and M. Kumar, "Deposition of Doped TiO₂ Thin Film by Sol Gel Technique and its Characterization", *Proceedings of the World Congress on Engineering*, Vol II, 2011.
- [5] Shukur H. A., Sato M., Nakamura I., and Takano I., "Characteristics and Photocatalytic Properties of TiO₂ Thin Film Prepared by Sputter Deposition and Post-N⁺ Ion Implantation", *Advances in Materials Science and Engineering*, Volume 2012, 1-8, 2012.
- [6] Nam S-H., Cho S-J. and Boo J-H., "Growth Behavior of Titanium Dioxide Thin Films at Different Precursor Temperatures", *Nanoscale Research Letters*, 7:89, 2012.
- [7] Bernardi M. I. B., Lee E. J. H., Lisboa-Filho P. N., Leite E. R., Longo E., Souza A. G., "Influence of the Growth Parameters on TiO₂ Thin Films Deposited Using the MOCVD Method", *Cerâmica*, Vol. 48 (308), 192-198, 2002.
- [8] Elfanaoui A., Ihlal A., Taleb A., Boukaddat L., Elhamri E., Meddah M., Bouabid K. and Portier X., "The Synthesis of TiO₂ Thin Film by Chemical Bath Deposition (CBD) Method", *MJCM*, VOLUME 13, No. 3, 2011.
- [9] Toma F-L., Bertrand G., Klein V., Meunier C., and Begin S., "Development of Photocatalytic Active TiO₂ Surfaces by Thermal Spraying of Nanopowders", *Journal of Nanomaterials* Volume 10, Article ID 384171, 8 pages, 2008.
- [10] Cao J., Sun J.-Z., Li H.-Y., Hong J., and Wang M., "A facile Room-Temperature Chemical Reduction Method to TiO₂@CdS Core/Sheath Heterostructure Nanowires", *J. Mater. Chem.*, 14, 1203 – 1206, 2004.
- [11] Zhu Y., Wang R., Zhang W., Ge H., Li L., "CdS and PbS Nanoparticles Co-Sensitized TiO₂ Nanotube Arrays and their Enhanced Photoelectrochemical Property", *ELSEVIER, Applied Surface Science* 315,p.p.149–153, 2014.
- [12] Baraton M-I., "Nano-TiO₂ for Solar Cells and Photocatalytic Water Splitting: Scientific and Technological Challenges for Commercialization", *The Open Nanoscience Journal*, Vol. 5, 64-77, 2011.
- [13] Das K., and De S. K., "Optical Properties of the Type-II Core-Shell TiO₂@CdS Nanorods for Photovoltaic Applications", *J. Phys. Chem. C*, 113, 3494–3501, 2009.
- [14] Patil U.M., Gurava K.V., Joob O-S., Lokhande C.D., "Synthesis of Photosensitive Nanograined TiO₂ Thin Films by SILAR Method", *ELSEVIER, Journal of Alloys and Compounds*, 478, 711–715, 2009.
- [15] Perillo P. M., Rodríguez D. F., "Formation of TiO₂ Nanopores by Anodization of Ti-Films", *Open Access Library Journal*, 1, 1-9, 2014.
- [16] Yu L., Wang D., and Ye D., "CdS Nanoparticles Decorated Anatase TiO₂ Nanotubes with Enhanced Visible Light Photocatalytic Activity", *ELSEVIER, Separation and Purification Technology*, 156,708-714, 2015.
- [17] Sahdan M. Z., Nayan N., Dahlan S. H., Mahmoud M. E., and Hashim U., "Sol-Gel Synthesis of TiO₂ Thin Films from In-House Nano-TiO₂ Powder", *Advances in Materials Physics and Chemistry*, Vol. 2, 16-20, 2012.
- [18] Lingeswaran K., Prasad Karamcheti S.S., Gopikrishnan M., and Ramu G., "Preparation and Characterization of Chemical Bath Deposited CdS Thin Film for Solar Cell", *Middle-East Journal of Scientific Research*, 20 (7): 812-814, 2014.